DOI: 10.24352/UB.OVGU-2019-002 TECHNISCHE MECHANIK, 39, 1, (2019), 3 – 15
submitted: September 4, 2018

Ferrofluid Flow in the Presence of Magnetic Dipole

G. Bognár, K. Hriczó

The aim of this paper is to introduce new results on magneto-thermomechanical interaction between heated viscous incompressible ferrofluid and a cold wall in the presence of a spatially varying magnetic field. Similarity transformation is applied to convert the governing nonlinear boundary layer equations into coupled nonlinear ordinary differential equations. This system is numerically solved using higher derivative method. The effects of governing parameters corresponding to various physical conditions are investigated. Numerical results are represented for distributions of velocity and temperature, for dimensionless wall skin friction and for heat transfer coefficients. Two bifurcate solutions have been obtained and one of the two solutions compares well with previous studies.

1 Introduction

During the last several decades, liquids are intensively investigated by various researchers due to their numerous applications in industry. One of them is the nanofluid, a homogenous combination of base fluid and nanoparticles. These suspensions are prepared with various metals or non-metals e.g., aluminium (Al), copper (Cu), silver (Ag), and graphite or carbon nanotubes respectively, and the base fluid, which includes water, oil or ethylene glycol, glycerol, etc. Ferrofluid is a special type of nanofluid. Magnetic fluids, also called ferrofluids, are stable colloidal suspensions of non-magnetic carrier liquid containing very fine magnetized particles, for example magnetite, with diameters of order 5-15 nm (see Papell (1965)). Ferrofluids are useful for retaining dust from the drive shafts of the magnetic disk drive. Furthermore, these fluids are used in enhancing the heat transfer rate in numerous materials and liquids in the industry.

Nanofluids can be used in many areas in our daily lives and technological processes. Such type of applications includes heat exchanger, vehicle cooling, nuclear reactor, cooling of electronic devices. The magneto nanofluids are also very much helpful in magnetic drug targeting in cancer diseases, hyperthermia, wound treatments, removal of blockage in the arteries, magnetic resonance imaging (MRI) etc. (see Bhatti et al. (2016)).

When magnetizable materials are subjected to an external magnetizing field **H**, the magnetic dipoles or line currents in the material will align and create a magnetization **M**.

Problem of magnetohydrodynamic (MHD) flow near infinite plate has been studied intensively by a number of researchers (see, e.g., Abel and Mahesha (2008), Adiguzel and Atalik (2017), Andersson and Valnes (1988), Bognár (2016a), Bognár (2016b), Siddheshwar and Mahabaleshwar (2005)). Andersson (1992) investigated the heat transfer rate in ferromagnetic fluids. The hydrodynamic flow of MHD fluids was studied when the applied transverse magnetic field is assumed to be uniform.

In recent years various theoretical models have been put forward to study the continuum description of ferrofluid flow. Most of the analytical studies concerning the motion of ferrofluids are based on the formulation given by either Neuringer and Rosensweig (1964) or Shliomis (2004). Neuringer and Rosensweig developed a model, where the effect of magnetic body force was considered under the assumption that the magnetization vector **M** is parallel to the magnetic field vector **H**.

Andersson and Valnes (1988) extended the so-called Crane's problem by studying the influence of the magnetic field, due to a magnetic dipole, on a shear driven motion, on a flow over a stretching sheet of a viscous non-conducting ferrofluid. It has been shown that the effect of the magnetic field is a slowing of the fluid movement compared to the hydrodynamic case. Abraham and Titus (2011) concluded that the presence of heat source (or sink) controls the effect of the magneto-thermomechanical interaction, which decelerates the flow along the stretching

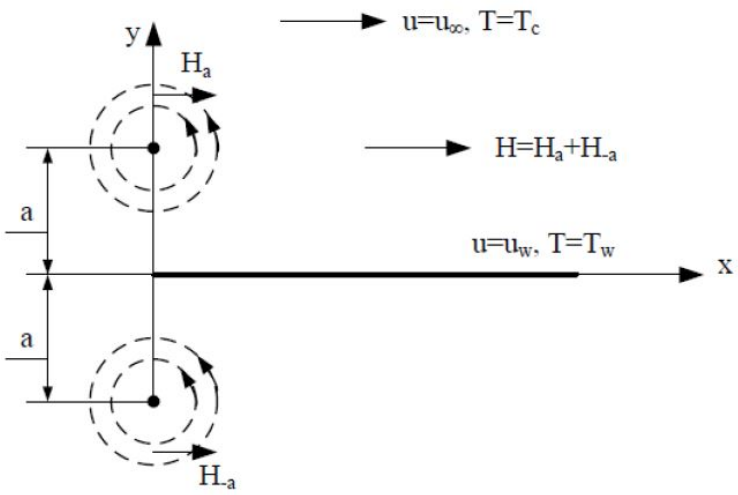

Figure 1: Parallel flow along a cold flat sheet in the presence of magnetic field due two line currents

sheet, thereby influence on the heat transfer rate. Zeeshan et al. (2016) investigated the effects of magnetic dipole and thermal radiation on the flow of ferromagnetic fluid on a stretching sheet.

Neuringer (1966) has examined numerically the dynamic response of ferrofluids to the application of non-uniform magnetic fields with studying the effect of magnetic field on two cases, the two-dimensional stagnation point flow of a heated ferrofluid against a cold wall and the two-dimensional parallel flow of a heated ferrofluid along a wall with linearly decreasing surface temperature.

The aim of this paper is to re-investigate the two-dimensional parallel flow of a heated ferrofluid along a wall with decreasing surface temperature of power-law type and the static behaviour of ferrofluids in magnetic field using similarity analysis. The similarity method is applied for the governing equations to transform partial differential equations to nonlinear ordinary differential equations. Numerical solutions are obtained with higher derivative method. The heat transfer, velocity and temperature distribution in the boundary layer are provided and compared with the results obtained by Neuringer (1966) for constant streaming speed and linearly decreasing wall temperature. The behaviour of the velocity and thermal distribution is presented. We point out for the existence of two different solutions on the base of numerical results to the corresponding boundary value problem. The effects of the parameters involved in the boundary value problem are graphically illustrated.

2 Problem Formulation

Consider a steady two-dimensional flow of an incompressible, viscous and electrically non-conducting ferromagnetic fluid over a flat sheet in the horizontal direction shown in Fig. 1.

The dipole of the magnet is placed at a distance a from the surface, in such a way its center lies on y-axis. The magnetic field (**H**) due to the magnetic dipole is directed towards positive x-direction. The ferrofluid influences by the dipole of the permanent magnet whose scalar potential is

$$\phi(x,y) = -\frac{I_0}{2\pi}\left(\tan^{-1}\frac{y+a}{x} + \tan^{-1}\frac{y-a}{x}\right), \tag{1}$$

where I_0 denotes the dipole moment per unit length and a is the distance of the line current from the leading edge. The wall temperature is a decreasing function of x and is given by $T_w = T_c - Ax^{m+1}$, where T_c denotes the Curie temperature, A and m are real constants.

The negative gradient of the magnetic scalar potential ϕ equals to the applied magnetic field, i.e. $\mathbf{H} = -\nabla\phi$.

Then, the corresponding field components are given by

$$H_x = -\frac{\partial \phi}{\partial x} = -\frac{I_0}{2\pi}\left[\frac{y+a}{x^2+(y+a)^2} + \frac{y-a}{x^2+(y-a)^2}\right], \tag{2}$$

$$H_y = -\frac{\partial \phi}{\partial y} = -\frac{I_0}{2\pi}\left[\frac{x}{x^2+(y+a)^2} + \frac{x}{x^2+(y-a)^2}\right]. \tag{3}$$

Moreover, the second derivatives are given by

$$\frac{\partial^2 \phi}{\partial x^2} = -\frac{\partial^2 \phi}{\partial y^2} = -\frac{I_0}{2\pi}\left[\frac{2x\,(y+a)}{\left[x^2+(y+a)^2\right]^2} + \frac{2x\,(y-a)}{\left[x^2+(y-a)^2\right]^2}\right] \tag{4}$$

and

$$\frac{\partial^2 \phi}{\partial x\,\partial y} = -\frac{I_0}{2\pi}\left[\frac{(y+a)^2-x^2}{\left[x^2+(y+a)^2\right]^2} + \frac{(y-a)^2-x^2}{\left[x^2+(y-a)^2\right]^2}\right]. \tag{5}$$

Neuringer and Rosensweig (1964) showed that the existence of spatially varying fields is required in ferrohydrodynamic interactions. We shall have the following assumptions for the exposition of ferrohydrodynamic interaction:

(i) the fluid temperature must be less than Curie temperature,

(ii) the applied magnetic field is inhomogeneous.

Then, the dynamic response of ferrofluids to the application of non-uniform magnetic fields follows from the fact that the force per unit volume on a piece of magnetized material of magnetization **M** (i.e. dipole moment per unit volume) in the field of magnetic intensity **H** is given by the form $\mu_0 M \nabla H$, where $H = \sqrt{\left(\frac{\partial \phi}{\partial x}\right)^2 + \left(\frac{\partial \phi}{\partial y}\right)^2}$, μ_0 denotes the free space permeability and M represents the magnitude of **M**. Applying the scalar potential ϕ, ∇H is calculated as follows

$$\nabla H = \left([\nabla H]_x, [\nabla H]_y\right) = \left(\frac{\frac{\partial \phi}{\partial x}\frac{\partial^2 \phi}{\partial x^2} + \frac{\partial \phi}{\partial y}\frac{\partial^2 \phi}{\partial x\,\partial y}}{\sqrt{\left(\frac{\partial \phi}{\partial x}\right)^2 + \left(\frac{\partial \phi}{\partial y}\right)^2}}, \frac{\frac{\partial \phi}{\partial x}\frac{\partial^2 \phi}{\partial x\,\partial y} + \frac{\partial \phi}{\partial y}\frac{\partial^2 \phi}{\partial y^2}}{\sqrt{\left(\frac{\partial \phi}{\partial x}\right)^2 + \left(\frac{\partial \phi}{\partial y}\right)^2}}\right), \tag{6}$$

where $[\nabla H]_x$ and $[\nabla H]_y$ denotes the first and second components of ∇H, respectively. Since $(\partial\phi/\partial x)_{y=0} = 0$ and $\left(\partial^2\phi/\partial y^2\right)_{y=0} = 0$ at the wall, then $[\nabla H]_y$ vanishes.

In the boundary layer for regions close to the wall when distances from the leading edge large compared to the distances of the line sources from the plate, i.e. $x \gg a$, then one gets

$$[\nabla H]_x = -\frac{I_0}{\pi}\,\frac{1}{x^2}. \tag{7}$$

From the above said consideration of the flow analysis, the governing equations (conservation of mass, momentum and energy) of the boundary layer flow are formed according to the following assumptions (Neuringer (1966)):

(i) the intensity of magnetic field is strong enough to drench the magnetic fluid, and the variation of magnetization M is the linear function of temperature as reported by $M = K(T_c - T)$, where K is the pyromagnetic coefficient and T_c denotes the Curie temperature proposed by Amirat and Hamdache (2012),

(ii) the induced field resulting from the induced magnetization compared to the applied field is neglected; hence, the ferrohydrodynamic equations are uncoupled from the electromagnetic equations and

(iii) in the temperature range to be considered, the thermal heat capacity c, the thermal conductivity k, and the coefficient of viscosity ν are independent of temperature.

Then, the governing equations are described as follows

$$\frac{\partial u}{\partial x}+\frac{\partial v}{\partial y}=0, \tag{8}$$

$$u\frac{\partial u}{\partial x}+v\frac{\partial u}{\partial y}=-\frac{I_o\mu_0 K}{\pi\rho}(T_c-T)\frac{1}{x^2}+\nu\frac{\partial^2 u}{\partial y^2}, \tag{9}$$

$$c\left[u\frac{\partial T}{\partial x}+v\frac{\partial T}{\partial y}\right]=k\frac{\partial^2 T}{\partial y^2}, \tag{10}$$

where the x and y axes are taken parallel and perpendicular to the plate, u and v are the parallel and normal velocity components to the plate, respectively, μ_0 means the permeability of the vacuum, ν is the kinematic viscosity and ρ denotes the density of the ambient fluid, which will be assumed constant. Equations (8)-(10) are considered under the boundary conditions at the surface ($y=0$) with

$$u(x,0)=0, \qquad v(x,0)=0, \qquad T(x,0)=T_w, \tag{11}$$

where $T_w=T_c-Ax^{m+1}$ and as y leaves the boundary layer ($y\to\infty$) with

$$u(x,y)\to u_\infty, \qquad T(x,y)\to T_\infty \tag{12}$$

where $T_\infty=T_c$, and u_∞ is the exterior streaming speed which is assumed throughout the paper to be $u_\infty=U_\infty x^m$ ($U_\infty=const.$). Parameter m is relating to the power law exponent. The parameter $m=0$ refers to a linear temperature profile and constant exterior streaming speed. In case of $m=1$, the temperature profile is quadratic and the streaming speed is linear. The value of $m=-1$ corresponds to no temperature variation on the surface.

Introducing the stream function ψ, defined by $u=\partial\psi/\partial y$ and $v=-\partial\psi/\partial x$, problem (8)–(10) can be formulated as

$$\frac{\partial\psi}{\partial y}\frac{\partial^2\psi}{\partial yx}-\frac{\partial\psi}{\partial x}\frac{\partial^2\psi}{\partial yy}=\nu\frac{\partial^3\psi}{\partial yyy}-\frac{I_0\mu_0 K}{\pi\rho}\left(T_c-T\right), \tag{13}$$

$$c\left[\frac{\partial\psi}{\partial y}\frac{\partial T}{\partial x}-\frac{\partial\psi}{\partial x}\frac{\partial T}{\partial y}\right]=k\frac{\partial^2 T}{\partial yy}. \tag{14}$$

Boundary conditions (11) and (12) are transformed to

$$\frac{\partial}{\partial y}\psi(x,0)=0, \qquad \frac{\partial}{\partial x}\psi(x,0)=0, \qquad T(x,0)=T_c-Ax^{m+1}, \tag{15}$$

$$\frac{\partial}{\partial y}\psi(x,y)\to U_\infty x^m \qquad T(x,y)=T_c \qquad \text{as } y\to\infty. \tag{16}$$

Using the following transformations, the structure of (13)–(16) allows us to look for similarity solutions of a class of solutions ψ and T in the form (see Barenblatt (1996))

$$\psi(x,y)=C_1x^b f(\eta), \qquad T=T_c-Ax^{m+1}\Theta\left(\eta\right), \qquad \eta=C_2x^d y, \tag{17}$$

where b and d satisfy the scaling relation

$$b+d=m \tag{18}$$

and for positive coefficients C_1 and C_2 the relation

$$\frac{C_1}{C_2}=\nu \tag{19}$$

are fulfilled. The real numbers b, d are such that $b - d = 1$ and $C_1 C_2 = U_\infty$, i.e.

$$b = \frac{m+1}{2}, \qquad d = \frac{m-1}{2}, \qquad C_1 = \sqrt{\nu U_\infty}, \qquad C_2 = \sqrt{\frac{U_\infty}{\nu}}. \tag{20}$$

By taking into account (17), equations (13) and (14) and conditions (15) and (16) lead to the following system of coupled ordinary differential equations

$$\frac{d^3 f}{d\eta^3} - m \left(\frac{df}{d\eta}\right)^2 + \frac{m+1}{2} f \frac{df}{d\eta} - \beta \Theta = 0, \tag{21}$$

$$\frac{d^2 \Theta}{d\eta^2} + (m+1) \, \mathrm{Pr} \left(\frac{1}{2} f \frac{d\Theta}{d\eta} - \Theta \frac{df}{d\eta}\right) = 0. \tag{22}$$

The boundary conditions reduces to the following equations subjected to the boundary conditions

$$f(0) = 0, \qquad \frac{d}{d\eta} f(0) = 0, \qquad \Theta(0) = 1, \tag{23}$$

$$\frac{d}{d\eta} f(\eta) = 1, \qquad \Theta(\eta) = 0 \qquad \text{as } \eta \to \infty, \tag{24}$$

where $\mathrm{Pr} = c\nu/k$ is the Prandtl number and $\beta = I_0 \mu_0 K A/(\pi \rho U_\infty^2)$.

The components of the non-dimensional velocity $\mathbf{v} = (u, v, 0)$ can be expressed by

$$u = U_\infty \, x^m \, \frac{df(\eta)}{d\eta}, \tag{25}$$

$$v = -\sqrt{\nu U_\infty} \, x^{(m-1)/2} \left(\frac{m+1}{2} f(\eta) + \frac{m-1}{2} \frac{df(\eta)}{d\eta} \eta\right). \tag{26}$$

The physical quantities that specify the surface drag and heat transfer rate can be derived. Mathematically these quantities are interpreted in the following form

$$\tau_{y=0} = \nu \rho \left(\frac{\partial u}{\partial y}\right)_{y=0} = \rho U_\infty \sqrt{\nu U_\infty} \, x^{\frac{3m-1}{2}} \frac{d^2}{d\eta^2} f(0), \tag{27}$$

$$-k \left(\frac{\partial T}{\partial y}\right)_{y=0} = -kA \sqrt{\frac{U_\infty}{\nu}} x^{\frac{3m+1}{2}} \frac{d}{d\eta} \Theta(0), \tag{28}$$

where $(d^2 f/d\eta^2)(0)$ denotes the skin friction coefficient and $(d\Theta/d\eta)(0)$ stands for the heat transfer coefficient.

According to our knowledge, the coupled boundary-layer equations for the case when $m = 0$ were first examined by Neuringer (1966). If $m = 0$ and $\beta = 0$, equation (21) is equivalent to the famous Blasius equation

$$\frac{d^3 f}{d\eta^3} + \frac{1}{2} f \frac{df}{d\eta} = 0, \tag{29}$$

which appears when studying a laminar boundary-layer problem for Newtonian fluids (see Barenblatt (1996)).

In the mathematical study of a model describing the dynamics of heat transfer in an incompressible magnetic fluid under the action of an applied magnetic field, the fluid is assumed nonelectrically conducting and the obtained solutions are valid only for distances greater than a.

3 Results and Discussion

There are several methods for the numerical solution of boundary value problems of similar type of coupled strongly nonlinear differential equations as (21)–(22). Bhatti et al. (2016) applied the successive linearization method to solve the boundary value problem, where the unknown functions are obtained by iteratively solving the linearized version of the governing equation. Using a selection of initial guesses, auxiliary linear operators are quite essential to find the homotopic solutions for flow analysis (see Hayat et al. (2015)). Tzirtzilakis and Kafoussias (2003) obtained numerical results by a numerical technique based on the common finite difference method. Zeeshan et al. (2016) and Abraham and Titus (2011) solved the highly non-linear differential equation subjected to boundary conditions by shooting method when the higher-order ordinary differential equations are converted into the set of first-order simultaneous equations, which can be integrated as an initial value problem using the well known Runge-Kutta Fehlberg fourth-order scheme. The initial guesses for the unknown functions were adjusted iteratively by Newton-Raphson's method.

Due to the difficulties involved in two-point boundary value problems, several researchers have explored different approaches for solving these types of problems. The differential transformation method has been proved to be effective to provide approximate analytical solutions as it does not require many computations as carried out in Adomian decomposition method (ADM), homotopy analysis method (HAM), homotopy perturbation method (HPM), and variational iteration method (VIM). Also, the differential transformation method introduced by Zhou (1986) has been used in many engineering and scientific research papers due to its comparative advantages over the other approximate analytical methods. These numerical method could be used to solve differential equations, difference equation, differential-difference equations, fractional differential equation, pantograph equation and integro-differential equation, to solves nonlinear integral and differential equations without restrictive assumptions, perturbation and discretization or round-off error.

The system of equations (21)–(22) with the corresponding conditions (23)–(24), is interpreted numerically using BVP solution technique built in Maple.

In this paper, the coupled ordinary differential equations (21)–(22) are solved numerically with boundary conditions using a special type of BVP technique, namely, the higher derivative method (HDM) with A-stability property. The HDM method can be applied for the determination of efficient solution to some boundary value problems, which are described by nonlinear ordinary differential equations (see Chen et al. (2017)). The discretization of boundary value problems based on HDM scheme. It is experienced that most of the test runs quickly, in a few seconds. The Maple code is attached in the Appendix.

During our investigations, the velocity and temperature changes in the boundary layer are examined and the effects of the parameters on the solution are illustrated on the figures.

The boundary value problems can have the situation that either no solution or multiple solutions exist even for the simple set of differential equations (see Bognár (2012) and Hussaini and Lakin (1986)). Here, the boundary value problem in Maple with applying the HDM method was solved. From the implementations we realized that two differential solutions exist, call them an upper and a lower solutions for velocity distribution, these are denoted by green and yellow curves and exhibited on Fig. 2 for $m = 0$, $Pr = 10$, $\beta = 0.1$ and for the length of $\eta_{max} = 6$. The Prandtl number $Pr = 10$ is fixed as a typical value of kerosine based ferrofluid. The obtained solutions of thermal distribution can be seen on Fig. 3, where we have lower and upper solutions, same as in the case of velocity, but in this case, the lower solution is in a good agreement with published by Neuringer (1966).

The ferromagnetic parameter β highlights the effect of the external magnetic field. The variation of β is shown on Figs. 4-5. It is can also be noticed that the boundary layer thickness is different for different values of β. The thermal boundary-layer thickness is smaller than the corresponding velocity boundary-layer thickness.

The effect of parameter m is presented in Fig. 6 for the shear stress at the wall, and the impact on the heat transfer at the wall in Fig. 7. It can be checked from the figures that for the increasing values of m the surface shear stress $f''(0)$ decreases, and the effect is opposite for the heat transfer rate $\Theta'(0)$.

Figure 8 shows the dependence of temperature profiles on the Prandtl number. Greater values of Pr result in thinning of thermal boundary layers. It is observed that an increasing in the Prandtl number decreases the temperature profile in the flow region.

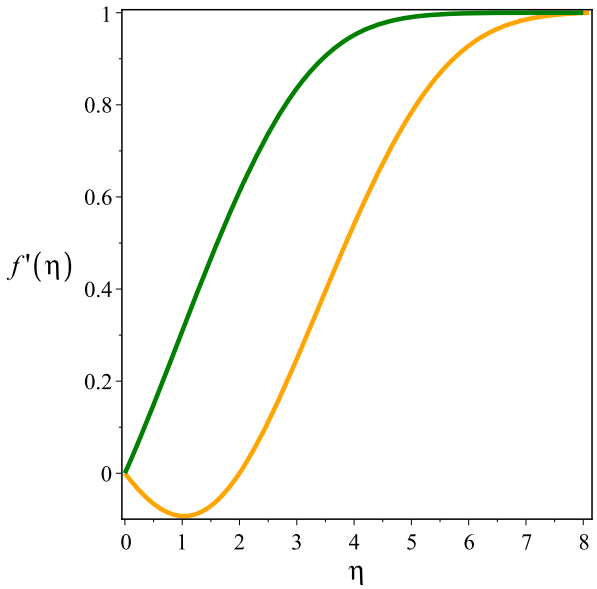

Figure 2: The effect of β on the velocity distribution for $m = 0$, $Pr = 10$, $\beta = 0.1$

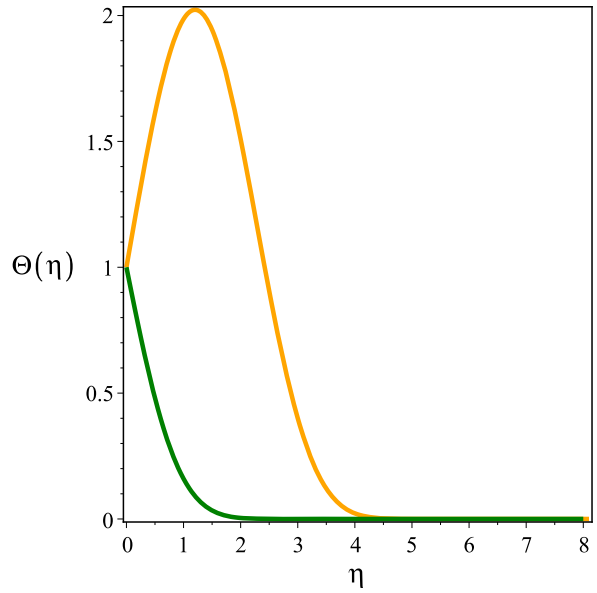

Figure 3: The effect of β on the temperature distribution for $m = 0$, $Pr = 10$, $\beta = 0.1$

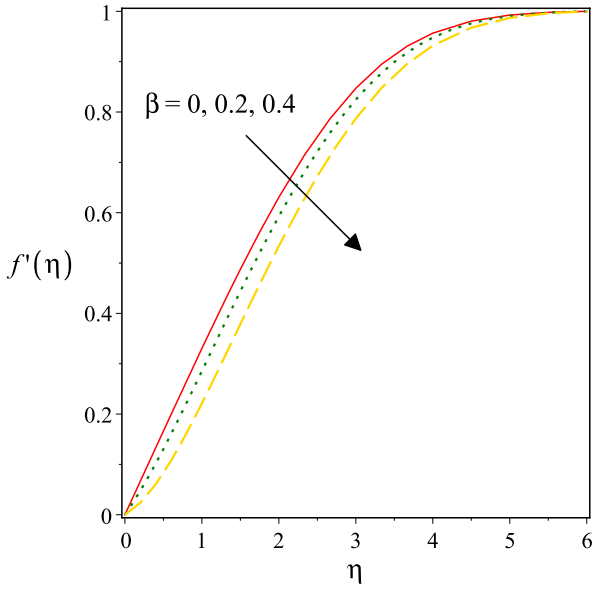

Figure 4: The velocity distribution for varying β ($m = 0$, $Pr = 10$)

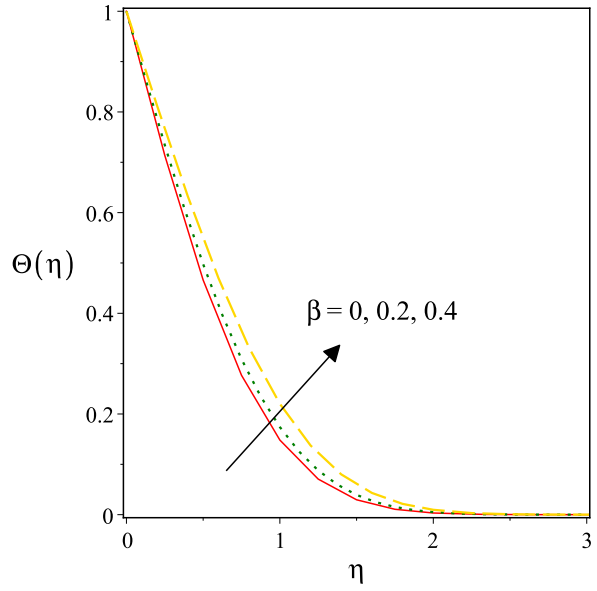

Figure 5: The temperature distribution for varying β ($m = 0$, $Pr = 10$)

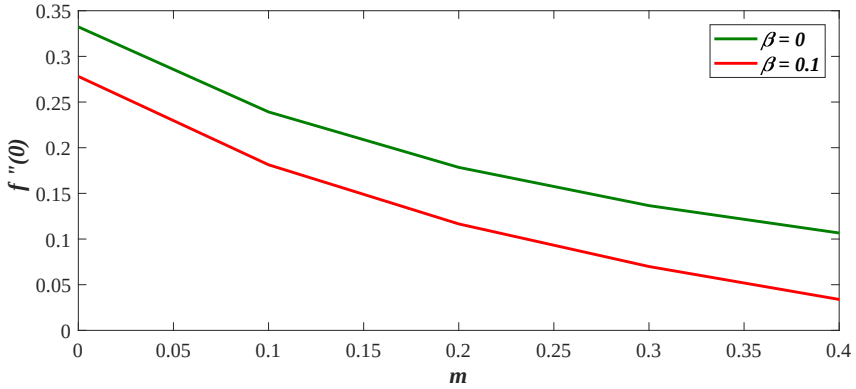

Figure 6: The shear stress at the wall for $Pr = 10$, $\beta = 0$ and $\beta = 0.1$

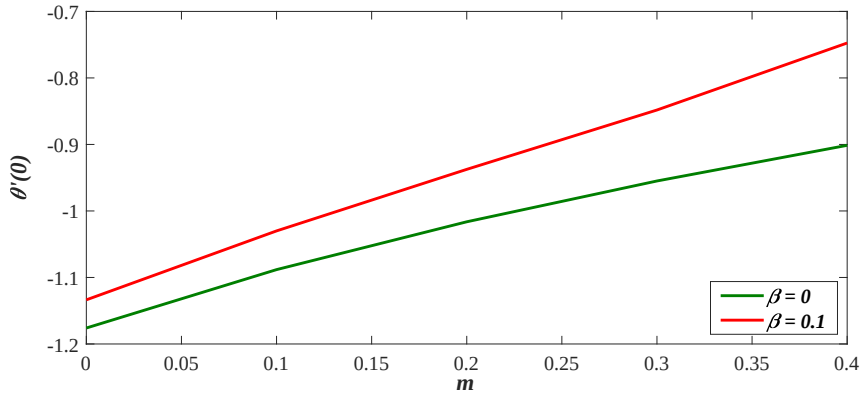

Figure 7: The heat transfer at the wall for $Pr = 10$, $\beta = 0$ and $\beta = 0.1$

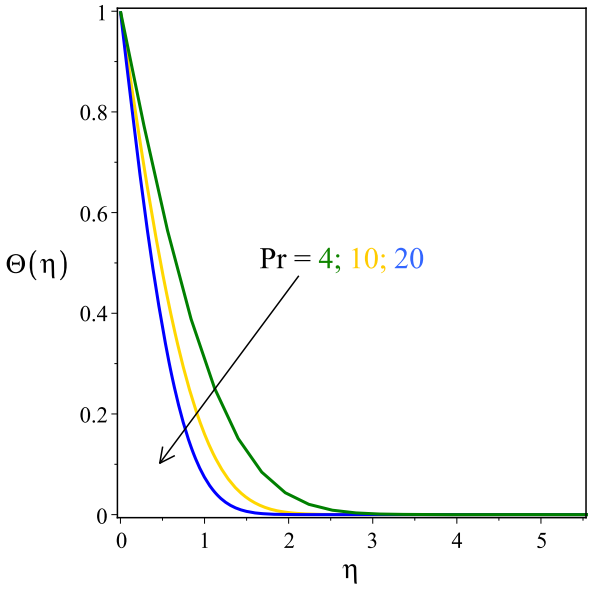

Figure 8: The effect of the Prandtl number $m = 0$ and $\beta = 0.1$

4 Conclusions

This paper presents similarity solution of the boundary layer flow and heat transfer over a cold wall of a ferrofluid fow in the presence of spatially varying magnetic field. By means of similarity transformation, the governing mathematical equations are reduced into ordinary differential equations which are then solved numerically using a higher derivative method. The effects of some governing parameters namely ferromagnetic parameter β, Prandtl number and power law parameter on the flow, and heat transfer characteristics are graphically presented and discussed. The findings of the numerical results can be summarized as follows:

(i) Dual solutions exist for the system of equations (21)–(22) with the corresponding conditions (23)–(24).

(ii) The effect of the external magnetic field is shown by he ferromagnetic parameter β. The boundary layer thickness is different for different values of β. The thermal boundary-layer thickness is smaller than the corresponding velocity boundary-layer thickness.

(iii) The increasing of parameter m is to decrease the surface shear stress $f''(0)$, and the effect is opposite for the heat transfer rate $\Theta'(0)$ on the wall.

(iv) The increase of the Prandtl number leads to a decrease of the temperature profile in the flow region.

Acknowledgements

This work was supported by project no. 129257 implemented with the support provided from the National Research, Development and Innovation Fund of Hungary, financed under the $K-18$ funding scheme.

Nomenclature

a	$[m]$	distance
A	$[K*m^{-(m+1)}]$	coefficient
c	$[J/K]$	thermal heat capacity
C_1, C_2	[-]	parameters
f	[-]	similarity velocity function
H	$[A/m]$	magnetic field strength
I_0	$[A]$	dipole moment per unit length
k	$[W/mK]$	thermal conductivity
K	$[A/mK]$	pyromagnetic coefficient
m	[-]	constant
M	$[A/m]$	magnetisation of the field
T	$[K]$	temperature
T_c	$[K]$	Curie temperature
T_w	$[K]$	wall temperature
T_∞	$[K]$	fluid temperature far from the wall
u_∞	$[m/s]$	fluid velocity
u, v	$[m/s]$	velocity components
u_w	$[m/s]$	wall velocity
x, y	$[m]$	distances parallel and perpendicular to the wall, respectively

Greek symbols

η	[-]	similarity variable
Θ	[-]	similarity temperature function
μ_0	$[Vs/Am]$	permeability of the vacuum
ν	$[m^2/s]$	kinematic viscosity
ρ	$[kg/m^3]$	density of the fluid
ϕ	$[A]$	scalar potential
ψ	$[m^2/s]$	stream function

References

Abel, M. S.; Mahesha, N.: Heat transfer in MHD viscoelastic fluid flow over stretching sheet with variable thermal conductivity, non-uniform heat source and radiation. *Appl. Math. Modelling*, 32, (2008), 1965–1983.

Abraham, A.; Titus, L. S. R.: Boundary layer flow of ferrofluid over a stretching sheet in the presence of heat source/sink. *Mapana J. Sci.*, 10, (2011), 14 – 24.

Adiguzel, A. B.; Atalik, K.: Magnetic field effects on Newtonian and non-Newtonian ferrofluid flow past a circular cylinder. *Appl. Math. Modelling*, 42, (2017), 161 – 174.

Amirat, Y.; Hamdache, K.: Heat transfer in incompressible magnetic fluid. *J. Math. Fluid Mech.*, 14, (2012), 217 – 247.

Andersson, H. I.: MHD flow of a viscoelastic fluid past a stretching surface. *Acta Mechanica*, 95, (1992), 227 – 230.

Andersson, H. I.; Valnes, O. A.: Flow of a heated ferrofluid over a stretching sheet in the presence of a magnetic dipole. *Acta Mechanica*, 128, (1988), 39 – 47.

Barenblatt, G.: *Scaling, self-similarity, and intermediate asymptotics: dimensional analysis and intermediate asymptotics*. Cambridge University Press, Cambridge, MA (1996).

Bhatti, M. M.; Abbas, T.; Rashidi, M. M.: Numerical study of entropy generation with nonlinear thermal radiation on magnetohydrodynamics non-newtonian nanofluid through a porous shrinking sheet. *J. Magnetics*, 21, (2016), 468 – 475.

Bognár, G.: On similarity solutions to boundary layer problems with upstream moving wall in non-Newtonian power-law fluids. *IMA J. Appl. Math.*, 77, (2012), 546 – 562.

Bognár, G.: Magnetohydrodynamic flow of a power-law fluid over a stretching sheet with a power-law velocity. *Differential and Difference Equations with Applications (Springer Proceedings in Mathematics and Statistics; 164. ICDDEA, Amadora, Portugal, 2015)*, pages 131 – 139.

Bognár, G.: On similarity solutions of MHD flow over a nonlinear stretching surface in non-Newtonian power-law fluid. *Electron. J. Qual. Theory Differ. Equ.*, 2016, (2016b), 1 – 12.

Chen, J.; Sonawane, D.; Mitra, K.; Subramanian, V. R.: Yet another code for boundary value problems- higher derivative method. *manuscript*.

Hayat, T.; Muhammad, T.; Shehzad, S. A.; Alsaedi, A.: Similarity solution to three dimensional boundary layer flow of second grade nanofluid past a stretching surface with thermal radiation and heat source/sink. *AIP Advances*, 5, 1, (2015), 017107.

Hussaini, M. Y.; Lakin, W. D.: Existence and nonuniqueness of similarity solutions of a boundary-layer problem. *Quart. J. Mech. Appl. Math.*, 39, (1986), 177 – 191.

Neuringer, J. L.: Some viscous flows of a saturated ferrofluid under the combined influence of thermal and magnetic field gradients. *J. Non-linear Mech.*, 1, (1966), 123 – 127.

Neuringer, J. L.; Rosensweig, R. E.: Ferrohydrodynamics. *Phys. Fluids*, 7, (1964), 1927 – 1937.

Papell, S. S.: Low viscosity magnetic fluid obtained by colloidal suspension of magnetic particles. *U.S. Patent*, 3, (1965), 3,215,572.

Shliomis, M.: Comment on ”ferrofluids as thermal ratchets”. *Phys. Rev. Lett.*, 92, (2004), 188901.

Siddheshwar, P. G.; Mahabaleshwar, U. S.: Effect of radiation and heat source on mhd flow of a viscoelastic liquid and heat transfer over a stretching sheet. *Int. J. Non-Linear Mech.*, 40, (2005), 807 – 820.

Tzirtzilakis, E. E.; Kafoussias, N. G.: Biomagnetic fluid flow over a stretching sheet with non-linear temperature dependant magnetization. *ZAMP*, 54, (2003), 551 – 565.

Zeeshan, A.; Majeed, A.; Ellahi, R.: Effect of magnetic dipole on viscous ferro-fluid past a stretching surface with thermal radiation. *J. Mol. Liq.*, 215, (2016), 549 – 554.

Zhou, J.: *Differential Transformation and Its Applications for Electrical Circuits*. Huazhong University Press, Wuhan, China (1986).

Address: University of Miskolc, Miskolc-Egyetemváros, Miskolc, H–3515, Hungary
email: v.bognar.gabriella@uni-miskolc.hu

Appendix

The HDM adapt procedure is applied to determine the approximate numeric solution. The simulation gives the value of unknown parameters B and C, and then we get the figure of all solution functions.

```
> restart:
> read("HDM.txt");
> Digits:=15;
> EqODEs:=[diff(y1(x),x) = y2(x),diff(y2(x),x) = y3(x),
diff(y3(x),x) = m*y2(x)*y2(x)-(m+1)/2*y1(x)*y3(x)+b*y4(x),
diff(y4(x),x) = y5(x),
diff(y5(x),x) = -Pr*((m+1)/2*y1(x)*y5(x)-(m+1)*y4(x)*y2(x))];
> bc1:=evalf([y1(x),y2(x),y3(x)-B,y4(x) - 1,y5(x)-C]);
> bc2:=evalf([y2(x)-1,y4(x)]);
> Range:=[0.,5.6];
> pars:=[m=0.00,beta=0.1,Pr=4];
> unknownpars:=[B,C]; nder:=5;nele:=20;
> atol:=1e-6;rtol:=atol/100;
> sol:= HDMadapt(EqODEs,bc1,bc2,pars,unknownpars,nder,nele,Range,atol,rtol):
> sol[1][(nops(sol[3])+1)*nops(EqODEs)+1..nops(sol[1])];
> sol[4];
> sol[5];
> NN:=nops(sol[3])+1; print(y5(x));
> node:=nops(EqODEs);

> odevars:=select(type,map(op,map(lhs,EqODEs)),'function');
> xx:=Vector(NN):
> xx[1]:=Range[1]:
> for i from 1 to nops(sol[3]) do xx[i+1]:=xx[i]+sol[3][i]:  od:
> for j from 1 to node do

> plot([seq([xx[i],rhs(sol[1][i+NN*(j-1)])],i=1..NN)],
axes=boxed,labels=[x,odevars[j]],style=point);

> end do;
```